2015-01-1225
Published 04/14/2015

doi:10.4271/2015-01-1225
saealtpow.saejournals.org

Synthesis of a Hybrid-Observer-Based Active Controller for Compensating Powetrain Backlash Nonlinearity of an Electric Vehicle during Regenerative Braking

Chen Lv, Junzhi Zhang, Yutong Li, and Ye Yuan
State Key Lab of ASE, Tsinghua Univ.

ABSTRACT

Regenerative braking provided by an electric powertrain is far different from conventional friction braking with respect to the system dynamics. During regenerative decelerations, the nonlinear powertrain backlash would excite driveline oscillations, deteriorating vehicle drivability and blended brake performance. Therefore, backlash compensation is worthwhile researching for an advanced powertrain control of electrified vehicles during regenerative deceleration.

In this study, a nonlinear powertrain of an electric passenger car equipped with a central motor is modeled using hybrid system approach. The effect of powertrain backlash gap on vehicle drivability during regenerative deceleration is analyzed. To further improve an electric vehicle's drivability and blended braking performance, an active control algorithm with a hierarchical architecture is studied for powertrain backlash compensation. Since the backlash in driveline is unable to be measured by a sensor, a high-level hybrid observer for backlash identification is designed at first. Then, based on the observation of the backlash traverse, a low-level switching-based active controller for powertrain backlash compensation is synthesized.

The proposed control algorithm is simulated and compared with a non-active baseline strategy under regeneration deceleration. The simulation results show that the nonlinear powertrain backlash is well compensated by the developed active control algorithm, and the vehicle drivability and blended braking performance are also significantly enhanced.

CITATION: Lv, C., Zhang, J., Li, Y., and Yuan, Y., "Synthesis of a Hybrid-Observer-Based Active Controller for Compensating Powetrain Backlash Nonlinearity of an Electric Vehicle during Regenerative Braking," *SAE Int. J. Alt. Power.* 4(1):2015, doi:10.4271/2015-01-1225.

INTRODUCTION

In urban driving situations, about one third to one half of the energy of the power plant is consumed during deceleration processes [1, 2]. As one of the key technologies of electric vehicle, a regenerative braking system, which has the ability to convert kinetic energy into electrical energy during decelerations, can effectively improve the energy efficiency of vehicle. Therefore, it has become a hot topic of research and development [3, 4, 5].

With respect to the system dynamics, regenerative braking provided by an electric powertrain is far different from conventional friction braking. Its introduction not only provides great potential for improving vehicle energy efficiency but also poses tremendous challenges to existing brake theories and control methods. Hence, it is of great importance to take the dynamic behaviour of the powertrain system into consideration in developing an advanced regenerative braking control strategy for electric vehicles.

Backlash, which introduces a hard nonlinearity into the powertrain control loop for torque generation and transmission, greatly affects the dynamic performance of a vehicle. The main source of backlash is play between gears in the final drive and the gearbox, but other plays throughout the drivetrain add to the backlash [6]. In an electric vehicle, when the driver quickly depresses and releases the accelerator pedal or vice versa, requesting a transition from acceleration to regenerative braking or vice versa, driveline backlash is first traversed, exciting the nonlinearity, and no torque is transmitted through the shaft during this period. After contact is achieved, the impact (referred to as shunt) leads to a large half-shaft torque, which, combined with the flexibility of the powertrain, causes the unexpected driveline oscillation (referred to as shuffle) [7].

The powertrain backlash oscillation problem and its solutions have been widely investigated for conventional vehicles. In [8], an engine torque profile shaping strategy was proposed to reduce drivetrain vibration for passenger cars. In [9], an anti-jerk controller of passenger cars was designed using H-infinity algorithm. However, for an electric vehicle, especially in the regenerative deceleration situations, the driveline oscillation problem becomes much tougher. The response of an electric motor is much faster than that of an internal combustion engine, and the motor's regenerative braking torque is usually far larger than that of engine braking in a conventional car, which results in more severe oscillations. Moreover,

during a process of blended regenerative and friction braking, the application of friction braking adds a disturbance to the load side, further affecting the backlash and increasing the complexity of oscillation compensation control. Therefore, powertrain backlash compensation is important for improving vehicle drivability and powertrain control performance during regenerative deceleration, and it is worthwhile researching. In [10], a shaking vibration control was developed for pure electric car Nissan Leaf. In [11], a feedback control system was implemented to compensate for the effect of the half-shaft dynamics. However, in the above studies, although the driveline oscillation caused by shaft flexibility was considered, the nonlinear backlash was neglected in favour of a linear model. Nevertheless, the backlash do exist in the real powertrain, and its effect on drivability of electric vehicles during regenerative braking have rarely been reported.

In this study, a nonlinear powertrain of an electric passenger car equipped with a central motor is modeled using hybrid system approach, i.e. the hybrid automaton. Effect of powertrain backlash gap on vehicle drivability during regenerative deceleration is analyzed. To further improve an electric vehicle's drivability and blended braking performance, an active control algorithm with a hierarchical architecture is studied for powertrain backlash compensation. Since the backlash in driveline is unable to be measured, i.e. the contact and backlash modes of a powertrain cannot be directly obtained by a sensor, a high-level hybrid observer for backlash identification is designed at first. Then, based on the observed backlash motion, a low-level switching-based active controller for powertrain backlash compensation is synthesized. The proposed control algorithm is simulated in the regenerative braking process and compared with two baseline situations. Simulation results show that the proposed active control can compensate the powertrain backlash well, improving the control performance of the half-shaft torque and vehicle drivability significantly.

HYBRID SYSTEM MODELING FOR NONLINEAR ELECTRIC POWERTRAIN

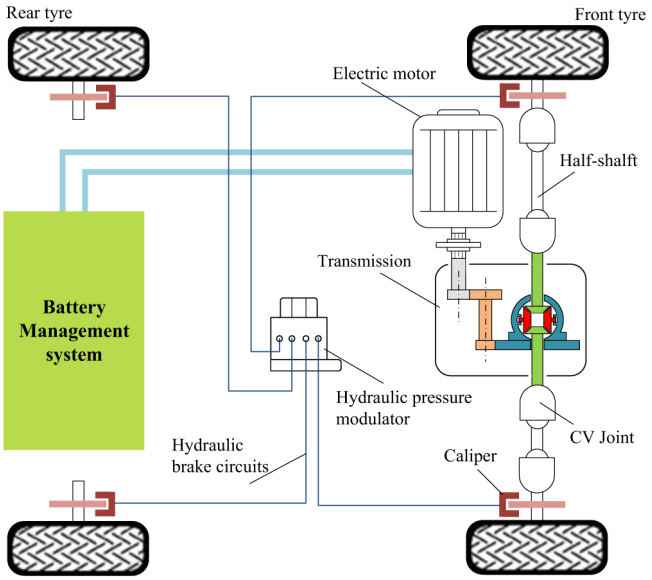

Figure 1. Overall structure of the blended braking system.

Figure 1 shows the overall structure of the regenerative and hydraulic blended braking system considered in this study. A central electric motor is installed at the front axle of the vehicle. During deceleration, regenerative braking torque transmitted by the driveline is exerted on the axle. In the meantime, friction braking torque is generated by the hydraulic modulator. The blended braking torque meets the overall braking demand. The electric powertrain, which comprises an electric motor, gearbox, final drive, differential, and half shafts, is modelled as described below.

Figure 2 shows a simplified two-inertia model of the electric powertrain used in this study. One inertia indicates the electric motor, and the other one represents the contribution of the wheel. The gearbox, consisting of the transmission, final drive, differential, and inner and outer constant-velocity (CV) joints, is located close to the motor inertia. The most important nonlinearity, which affects the driveline behaviour, is the backlash. The backlash contributions throughout the powertrain are lumped together into one single backlash angle, noted as 2α. The half shaft is modelled as a flexible one, representing its stiffness and damping properties. And the motor output torque is assumed to be equally distributed to the left and right half shafts.

Considering the effect of the electrical system dynamics, the motor torque is modelled as a first-order reaction [2], as shown in equation (1).

$$\tau_m \dot{T}_m(t) + T_m(t) = T_{m,ref}(t) \tag{1}$$

where $T_m(t)$ is the real value of motor torque and $T_{m,ref}(t)$ is the reference value.

The dynamic equation for the transmitted torque from the motor output shaft to the half shafts is as follows:

$$J_m \ddot{\theta}_m(t) + b_m \dot{\theta}_m(t) = T_m(t) - 2T_{hs}(t)/i_0 i_g \tag{2}$$

where J_m is the motor inertia, b_m is the viscous friction of the motor, $i_0 i_g$ is the transmission ratio, and $T_{hs}(t)$ is the half-shaft torque.

A flexible half shaft with nonlinear backlash connects the gearbox and the wheel inertia. The nonlinear model for the half-shaft torque can be given by [7]:

$$T_{hs}(t) = k_{hs}\theta_s(t) + c_{hs}\dot{\theta}_s(t) \tag{3}$$

$$\theta_s(t) = \theta_d(t) - \theta_b(t) \tag{4}$$

$$\theta_d(t) = \theta_1(t) - \theta_3(t),\ \theta_b(t) = \theta_2(t) - \theta_3(t) \tag{5}$$

where k_{hs} and c_{hs} are the stiffness and damping coefficients of the half shaft, respectively; $\theta_d(t)$ is the shaft twist angle; $\theta_b(t)$ is the backlash position; and $\theta_1(t)$, $\theta_2(t)$, and $\theta_3(t)$ are the angles at the indicated positions on the shaft, as shown in Figure 2,

where $\theta_1(t) = \theta_m(t)/i_0 i_g$ and $\theta_3(t) = \theta_w(t)$.

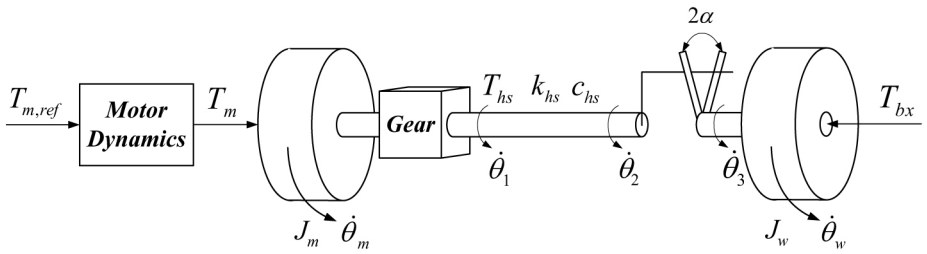

Figure 2. Two-inertia simplified model of electric powertrain system.

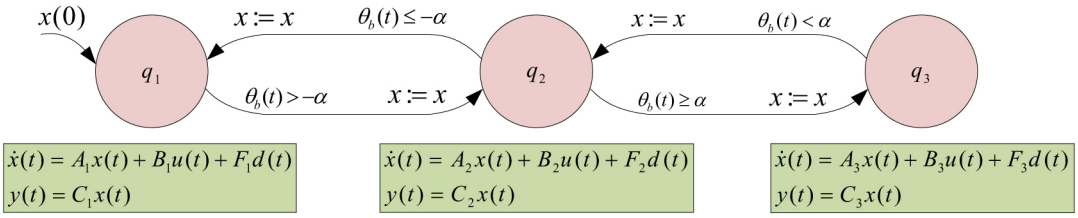

Figure 3. Hybrid automaton of electric powertrain system.

The nonlinear model for the backlash position is described by [6]:

$$\dot{\theta}_b(t) = \begin{cases} \max\left(0, \dot{\theta}_d(t) + \frac{k_{hs}}{c_{hs}}(\theta_d(t) - \theta_b(t))\right) & , \theta_b(t) = -\alpha \\ \dot{\theta}_d(t) + \frac{k_{hs}}{c_{hs}}(\theta_d(t) - \theta_b(t)) & , |\theta_b(t)| < \alpha \\ \min\left(0, \dot{\theta}_d(t) + \frac{k_{hs}}{c_{hs}}(\theta_d(t) - \theta_b(t))\right) & , \theta_b(t) = \alpha \end{cases} \quad (6)$$

where 2α is the backlash gap size.

The dynamic equation for a driven wheel is as follows:

$$J_w\ddot{\theta}_w(t) + b_w\dot{\theta}_w(t) = T_{hs}(t) - T_{hb}(t) - T_{bx}(t) \quad (7)$$

where J_w is the wheel inertia and the road load is divided into a friction part b_w and the tyre longitudinal force T_{bx}. The friction braking torque T_{hb}, generated by mechanical hydraulic brake devices, can be considered as a disturbance to the wheel.

Due to the piecewise affine dynamics of the backlash shown in equation (6), the system presents nonlinear characteristics. It is suitable to describe the powertrain dynamics using hybrid system approach, which is a powerful system modelling methodology.

Definition *A hybrid system* $\mathcal{H}$ is a collection:

$$\mathcal{H} = (Q, \sigma, \psi, X, U, D, Y, \text{Init}, f, h, R)$$

where

- Q is the finite set of discrete states;
- $X \subseteq \mathbb{R}^n$, $U \subseteq \mathbb{R}^p$, $D \subseteq \mathbb{R}^n$, and $Y \subseteq \mathbb{R}^p$ are the domains of continuous state, input, disturbance, and output variables, respectively;
- Init $\subseteq Q \times X$ is the set of initial states;
- $f : Q \times X \times U \times D \to TX$ and $h : Q \times X \to Y$ are the vector fields defining the dynamics of the continuous state and output variables, and TX is the tangent space to X;
- $R : Q \times Q \times X \to X$ describes the continuous state resets.

For an electric powertrain, if we define the contact as being positive when a half shaft is transmitting a driving torque, then the contact under regenerative deceleration is negative.

Based on the above definition of hybrid system, according to equations (1), (2), (3), (4), (5), (6), (7), the electric powertrain can be represented as:

- $Q = \{q_1, q_2, q_3\}$;
- $X = \{T_m, \theta_s, \dot{\theta}_m, \dot{\theta}_w, \theta_b\}$;
- $U = \{T_{m,\text{ref}}\}$;
- $D = \{T_{hb}, T_{bx}, T_l\}$;
- $Y = \{T_m, \dot{\theta}_m, \dot{\theta}_w\}$.

As the hybrid automaton shown in Figure 3, the system is comprised of three discrete states, namely, q_1, q_2, and q_3, indicating "*negative contact*", "*backlash traversing*", and "*positive contact*", respectively. And each discrete location has its own dynamics for continuous state variables' evolution. The continuous dynamics in each discrete state can be represented as:

$$\dot{x}(t) = A_i x(t) + B_i u(t) + F_i d(t)$$
$$y(t) = C_i x(t) \tag{8}$$

where A_i, B_i, C_i, and F_i in each location can be given by:

$$A_1 = A_3 = \begin{pmatrix} -\frac{1}{\tau_m} & 0 & 0 & 0 & 0 \\ 0 & -\frac{k_{hs}}{c_{hs}} & 0 & 0 & 0 \\ \frac{1}{J_m} & 0 & -\frac{b_m}{J_m} & 0 & 0 \\ 0 & 0 & 0 & -\frac{b_w}{J_w} & 0 \\ 0 & 0 & 0 & 0 & 0 \end{pmatrix} \quad A_2 = \begin{pmatrix} -\frac{1}{\tau_m} & 0 & 0 & 0 & 0 \\ 0 & -\frac{k_{hs}}{c_{hs}} & 0 & 0 & 0 \\ \frac{1}{J_m} & 0 & -\frac{b_m}{J_m} & 0 & 0 \\ 0 & 0 & 0 & -\frac{b_w}{J_w} & 0 \\ 0 & \frac{k_{hs}}{c_{hs}} & 1/i_0 i_g & -1 & 0 \end{pmatrix} \tag{9}$$

$$B_1 = B_2 = B_3 = \begin{pmatrix} \frac{1}{\tau_m} & 0 & 0 & 0 & 0 \end{pmatrix}^T \tag{10}$$

$$C_1 = C_2 = C_3 = \begin{pmatrix} 1 & 0 & 1 & 1 & 0 \end{pmatrix}^T \tag{11}$$

$$F_1 = F_3 = \begin{pmatrix} 0 & 0 & 0 \\ \frac{1}{c_{hs}} & 0 & \frac{1}{c_{hs}} \\ -\frac{2}{i_0 i_g J_m} & 0 & -\frac{2}{i_0 i_g J_m} \\ 0 & -\frac{1}{J_w} & \frac{1}{J_w} \\ 0 & 0 & 0 \end{pmatrix} \quad F_2 = \begin{pmatrix} 0 & 0 & 0 \\ 0 & 0 & 0 \\ 0 & 0 & 0 \\ 0 & -\frac{1}{J_w} & -\frac{1}{J_w} \\ 0 & 0 & 0 \end{pmatrix} \tag{12}$$

To simulate the brake blending processes, the hydraulic brake, the vehicle, and the tyre, has also been modelled in MATLAB/Simulink.

Details of these models were reported in references [4, 12, 13]. Their feasibility and effectiveness have been verified via hardware-in-the-loop tests and vehicle tests [2, 4, 14].

Some key parameters of the case study vehicle are listed in Table 1.

Table 1. Key parameters of the case-study electric vehicle.

Parameter	Value	Unit
Total mass (m)	1360	kg
Wheel base (L)	2.50	m
Frontal area (A)	2.40	m²
Coefficient of air resistance (C_D)	0.32	—
Nominal radius of tyre (r)	0.295	m

EFFECTS OF NONLINEAR BACKLASH ON ELECTRIC VEHICLE DRIVABILITY DURING REGENERATIVE BRAKING

For an electric vehicle, once it goes from driving mode to regenerative braking, the backlash is traversed, exciting the nonlinearity. In backlash mode, there is no torque being transmitted through the half shaft, and therefore the motor and the load are decoupled.

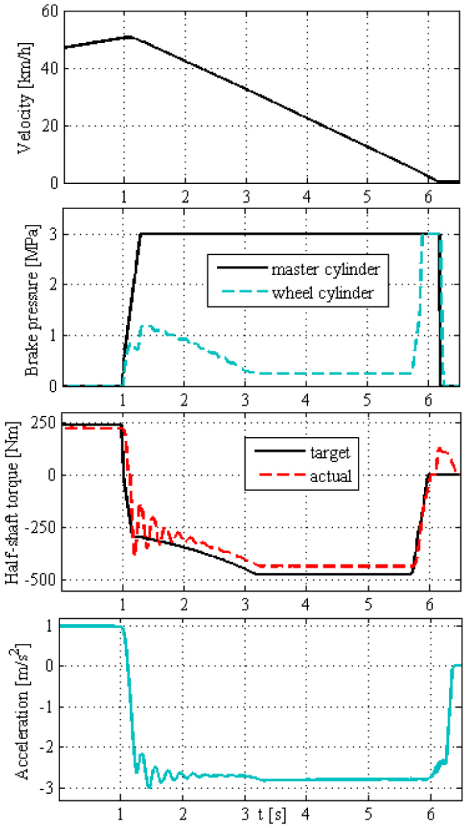

Figure 4. Simulation results of non-active baseline control algorithm.

Figure 4 illustrates the simulation results of powertrain state variables under non-active control in a torque transition process. Within 1st second, the vehicle is driven. At 1s, the drive depresses the brake pedal with the master cylinder pressure being increased, requesting a regenerative braking torque. Thus, a transition of torque from positive value to negative one occurs. As Figure 4 shows, at around 1.1 s, an unexpected torque oscillation occurs on the half shaft during the transition, and it results in an uncomfortable jerk in the vehicle's deceleration.

Focusing on this torque transition procedure, as Figure 5 shows, the backlash (BL) traverse happens at approximately 1.1 s, and the contact is changed from the positive side (CO+) to the negative side (CO-). During the backlash gap, since the motor and the load are decoupled, all the motor output torque is applied to its own inertia, which accelerates the motor significantly. Therefore, when the negative contact occurs, the speed difference between the motor and the load exceeds −2 rad/s. The large resulting impact (shunt) causes torque oscillations (shuffle) on the half shaft and an unexpected jerk

in vehicle deceleration. Thus, a controller that does not take traversing of the backlash into account will have a very difficult task damping the torque oscillations.

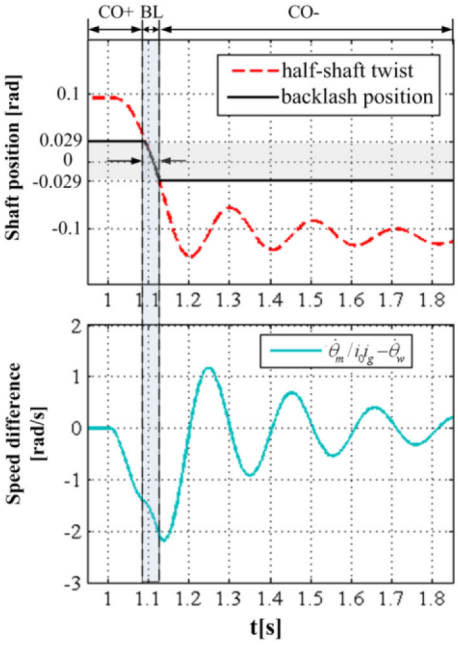

Figure 5. Simulation results during torque transition procedure.

HYBRID OBSERVER DESIGN

To further enhance the drivability of the electric vehicle during regenerative braking, an active controller for powertrain backlash compensation needs to be developed.

However, in the real world application, the backlash position and half-shaft torque are unable to be measured by sensors on the plant. Therefore, the development of an observer for unmeasurable states' estimation is necessary. To cope with the hybrid physical plant, a hybrid architecture is selected for the observer.

Definition *A hybrid observer* $\mathcal{H}_O$ [15] of a given hybrid system $\mathcal{H}$ such that

- receives, as discrete input $\sigma(k)$, the discrete output $\psi(k)$ of $\mathcal{H}$ and, as continuous input $u(t)$ and output $y(t)$ of $\mathcal{H}$;
- provides, as outputs estimates $\hat{q}(k)$ and $\hat{x}(t)$ of the current location $q(k)$ and continuous state $x(t)$ of the hybrid system $\mathcal{H}$, respectively.

As shown in Figure 6, the structure of the proposed hybrid observer $\mathcal{H}_O$ is composed of two blocks:

1. a discrete observer for location identification;
2. a continuous observer for the evolution of state variables.

The discrete observer receives as input the plant inputs (σ, u) and measured outputs (ψ, y), providing the estimation $\hat{q}$ of the discrete location of the hybrid plant at the current time. In the following sections, the location observer and the continuous observer are described in details.

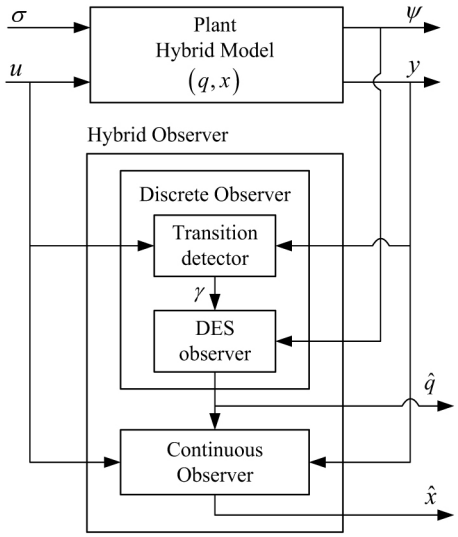

Figure 6. Structure of the proposed hybrid observer.

Here, we define a residual signal $r_i(t)$. When the hybrid system is in location q_i, the i-th residual generator produces a corresponding residual signal $r_i(t)$, which should converge to zero. A simple approach for this purpose is to use a Luenberger observer [15], tuned on the continuous dynamics associated to location q_i to be detected:

$$\dot{\hat{x}}(t) = (A_i - L_i C_i)\hat{x}(t) + B_i u(t) + L_i y(t)$$
$$r_i(t) = C_i \hat{x}(t) - y(t) \tag{13}$$

where L_i is a design parameter defining the converging rate of $r_i(t)$, and A_i, B_i, C_i are as in equations (9), (10), (11).

Then, the decision of the transition to i-th location can be made based on the evolution of $r_i(t)$. A simple implementation can be [16]:

$$\gamma_i(t) = \begin{cases} true & \text{if } \|r_i(t)\| \le \varepsilon \\ false & \text{if } \|r_i(t)\| > \varepsilon \end{cases} \tag{14}$$

where the threshold ε is a design parameter.

The above transition detector γ detects the transitions of the hybrid system $\mathcal{H}$ in between locations q1, q2, and q3, and then the discrete event system (DES) observer is able to correctly identify the current location of the hybrid system.

Continuous Observer Design

The continuous behaviour of the hybrid observer determines the evolution of the estimate $\hat{x}(t)$ of the system continuous state $x(t)$.

In each location $\hat{q}$, $\hat{x}(t)$ is associated to the continuous dynamics of the system [15]:

$$\dot{\hat{x}}(t) = \hat{f}\left(\hat{q}(k), \hat{x}(t), u(t), y(t)\right) \tag{15}$$

$$\hat{f} = (A_i - G_i C_i)\hat{x}(t) + B_i u(t) + G_i y(t) \tag{16}$$

where A_i, B_i, C_i are as in equations (9), (10), (11), and the observer gain G_i is the design parameter used to set the velocity of convergence in each location.

Note that both equation (13) and (16) provide estimation of state variable. However, these two evolutions are independent. Because the transition detector is expected to provide discrete information with fast transients regardless possible overshoots, while the continuous observer has to yield a smooth estimate of the state variables with good robustness [15]. This is the reason why another observer here in equation (16) is introduced.

ACTIVE CONTROLLER SYNTHESIS FOR POWERTRAIN BACKLASH COMPENSATION

Based on the system dynamics analyzed and observer designed above, an active controller is developed as follows for powertrain backlash compensation.

Backlash Mode Control

The goal of backlash control is to reduce the impact force of the motor on the load when contact is re-established, realizing a "soft landing" that avoids chatter. This can be accomplished by requiring the speed difference between the motor and the load sides to be small. Then, the backlash compensation can be seen as a speed tracking problem. The objective is to track the reference speed, which is the wheel speed in this study, with the motor speed.

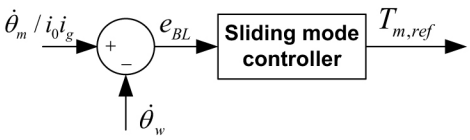

Figure 7. Structure of the backlash mode controller

Due to its ability to handle nonlinearity and achieve fast response, a sliding-mode control (SMC) scheme is adopted for the backlash controller, as Figure 7 shows. The error term is defined as:

$$e_{BL} = \dot{\theta}_m / i_0 i_g - \dot{\theta}_w \tag{17}$$

To guarantee zero steady error, an integral-type sliding surface is chosen. The sliding surface can be defined as:

$$S = e_{BL} + \lambda \int e_{BL} dt = 0 \tag{18}$$

For designing a control law that derives the system trajectories to the sliding surface, the Lyapunov direct method is used:

$$V = \frac{1}{2} SS \tag{19}$$

To ensure the stability of the system, the following condition needs to be satisfied:

$$\dot{V} = S\dot{S} \le 0 \tag{20}$$

If $S\dot{S} = -SKS$, where K is a positive constant, such that the above inequality can be satisfied. Hence,

$$S\dot{S} = -SKS \Rightarrow S(\dot{S} + KS) = 0 \tag{21}$$

Based on equation (18), the derivative of S can be expressed as:

$$\dot{S} = \ddot{\theta}_m / i_0 i_g - \ddot{\theta}_w + \lambda e \tag{22}$$

Combining equations (2) and (22), neglecting the electric motor's dynamics, and plugging $\dot{S}$ into $\dot{S} + KS = 0$, the following expression is obtained:

$$\ddot{\theta}_w - \frac{1}{i_0 i_g J_m} T_{m,ref} + \lambda e_{BL} + KS = 0 \tag{23}$$

Thus, the control input in backlash mode can be written as follows:

$$T_{m,ref} = T_{ref,BL} = i_0 i_g J_m \left(\ddot{\theta}_w + \lambda e_{BL} + KS\right) \tag{24}$$

During the blended braking process, the hydraulic brake, which exerts great impact on backlash control performance, also needs to be considered. To simplify the implementation, the wheel cylinder pressure is set to be maintained during the backlash phase, as shown in equation (25).

$$\dot{p}_{w,ref} = 0 \tag{25}$$

Contact Mode Control

After the backlash being traversed, in contact mode, the control objective is changed to track the target value of half-shaft torque with the real value. A combined feed-forward and feed-back control structure, as Figure 8 shows, is adopted:

$$T_{ref,CO} = T_{ff} + T_{fb} \tag{26}$$

where T_{ff} is the feed-forward input term required for tracking and T_{fb} is the feed-back component designed to reduce the control error.

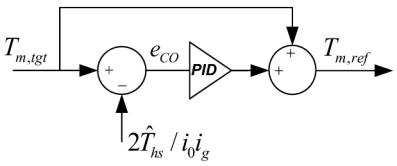

Figure 8. Structure of the contact mode controller.

Based on the control objective, the feed-forward term can be given by:

$$T_{ff} = T_{m,tgt} \tag{27}$$

$$T_{m,tgt} = \max(T_{b,f}, \frac{1}{i_0 i_g} T_{m,\lim}) \tag{28}$$

where $T_{m,tgt}$ is the target value of the motor torque, $T_{b,f}$ is the total brake demand of the front wheels, and $T_{m,lim}$ is the torque limit of the electric motor.

Since the value of half-shaft torque is unable to be measured by a sensor on-board, the estimation techniques have been studied by some researchers [17, 18]. In this work, based on the hybrid observer developed above, the estimate value of half-shaft torque $\hat{T}_{hs}$ can also be obtained. Then, in contact mode, the error term between the target and the observed value of half-shaft torque $\hat{T}_{hs}$ can be represented by:

$$e_{CO} = T_{m,tgt} - 2\hat{T}_{hs} / i_0 i_g \tag{29}$$

For the feedback component, a PID control law is adopted:

$$T_{fb} = K_P e_{CO} + K_I \int e_{CO} dt + K_D \frac{d}{dt} e_{CO} \tag{30}$$

where the feedback gains K_P, K_I, and K_D are tuning parameters.

To meet the overall braking demand of the vehicle in contact mode, the reference value of the hydraulic brake pressure is calculated based on the total brake demand of the front wheels, $T_{b,f}$, and the observed half-shaft torque $\hat{T}_{hs}$:

$$p_{w,ref} = k_0 (T_{b,f} - 2\hat{T}_{hs}) \tag{31}$$

where k_0 is the conversion coefficient between the wheel cylinder pressure and braking torque.

Based on the above discussion, an overall developed control protocol has a hierarchical architecture consisting of a high-level hybrid observer and a mode-switching-based active controller in the low-level, as shown in Figure 9.

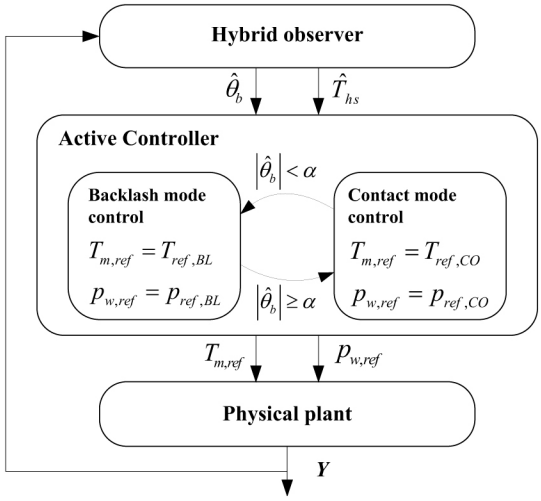

Figure 9. Hierarchical architecture of the proposed active controller

SIMULATIONS

To evaluate the control performance of the proposed algorithm during regeneration deceleration, simulations are carried out in MATLAB/ Simulink.

Simulation Scenario Set-Up

In the simulations, the initial braking speed is 40 km/h. The vehicle is powered within the first second, and then a brake torque is requested by the driver. The transition occurs from the positive contact (CO+) to the negative contact (CO-) side with backlash being traversed. The master cylinder pressure is taken as a ramp input stabilizing at 3 MPa. The road surface is assumed to be dry and has a high adhesion coefficient. The proposed active controller is simulated as follows.

Simulation Results of the Active Controller

Figure 10 and Figure 11 show the simulation results of active control for backlash compensation.

According to Figure 10, as with the active control discussed above, the half-shaft torque remains consistent with the target value. And during backlash mode at about 1.1s, the controller actively decreases the motor torque effort. The motor's regenerative brake torque is smoothly applied, and meanwhile, the value of the hydraulic brake pressure is maintained.

As a result, the speed difference between the motor and the wheel becomes smaller during the backlash gap. And the half-shaft position changes much more smoothly, as Figure 11 shows.

Comparison of the Proposed Algorithm with Baseline

In order to examine the control performance of the proposed active controller, the original scenario with non-active control is taken as a baseline. Its simulation results have been shown in Figures 4 and 5 in section 3. Besides, since the simple torque shaping, which limits the

torque change rate around zero crossing point, can be easily realized in vehicle application, hence it is added as another baseline to be compared against the proposed approach.

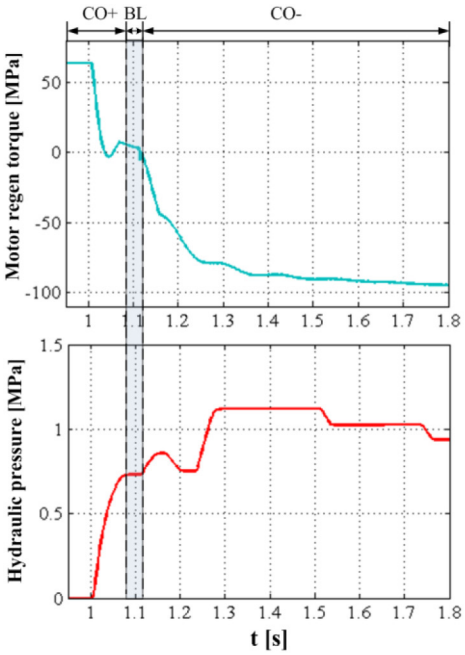

Figure 10. Simulation results of the motor torque and hydraulic brake pressure under the proposed active control algorithm.

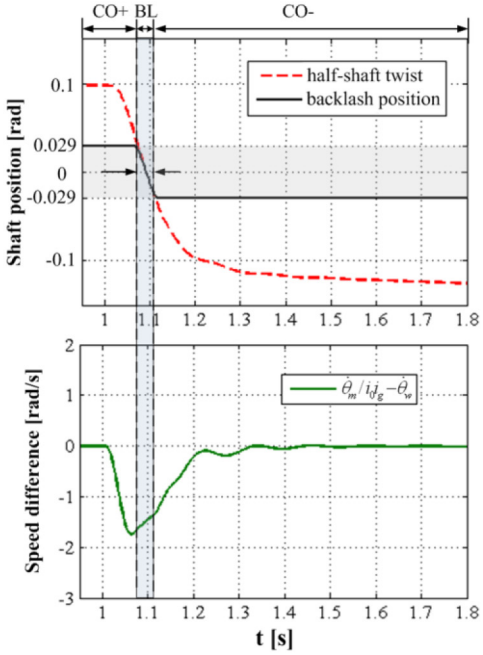

Figure 11. Simulation results of the half-shaft position and speed difference under the proposed active control algorithm.

Figure 12 illustrates that compared to the two baseline situations, the proposed active controller achieves good performance in half-shaft torque tracking and powertrain backlash compensation during transition process, resulting in a good vehicle drivability.

As shown in Table 2, the control effect of the half-shaft torque is evaluated quantitatively by the average tracking error. Besides, the root mean square error (RMSE) of jerk is selected as a parameter for evaluating vehicle drivability. The comparisons of RMSE of jerk under the two different strategies are also listed below.

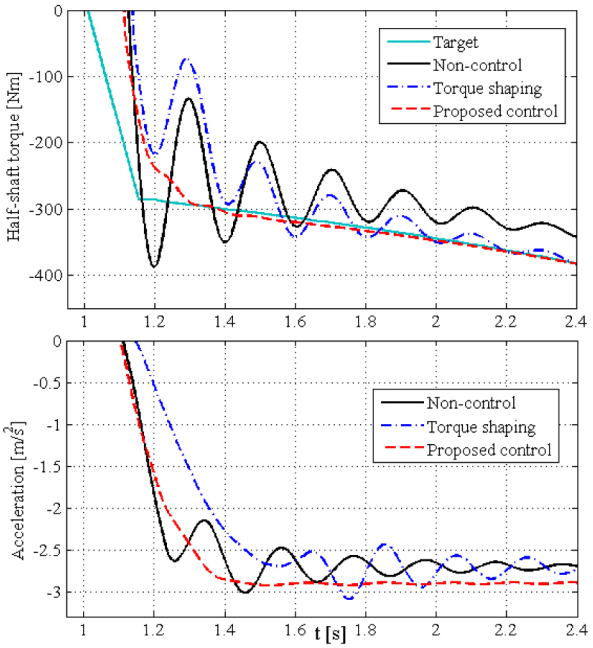

Figure 12. Drivetrain control performances and drivability under different control algorithms.

Table 2. Simulation results of control performance and vehicle drivability.

Control algorithm	Average tracking error	RMSE of jerk
Non-control	64.82 Nm	10.35 m/s^3
Torque shaping	45.29 Nm	7.07 m/s^3
Active control	21.05 Nm	3.38 m/s^3

CONCLUSIONS

During regenerative braking processes, powertrain backlash would excite driveline oscillations, deteriorating vehicle drivability and braking control performance. This paper investigated the active control of the powertrain for backlash compensation for an electric vehicle during regenerative deceleration. An electric powertrain model with backlash nonlinearity was developed using hybrid systems approach. The effect of powertrain backlash on vehicle drivability during regenerative deceleration was analysed. Since the backlash position in driveline is unable to be measured, a hybrid observer, which is comprised of a discrete and a continuous observer, is developed for backlash identification. To further improve the electric vehicle's drivability and blended braking performance, a switching-based active controller was developed. Simulations of the proposed algorithm under regenerative deceleration were carried out. The simulation results showed that the active control can well compensate the powertrain backlash, resulting in significant improvement in the control performance of the half-shaft torque and vehicle drivability.

REFERENCES

1. Gao, Y. and Ehsani, M., "Electronic Braking System of EV And HEV---Integration of Regenerative Braking, Automatic Braking Force Control and ABS," SAE Technical Paper 2001-01-2478, 2001, doi:10.4271/2001-01-2478.
2. Zhang, J.Z., Lv, C., Gou, J.F. and Kong, D.C., "Cooperative control of regenerative braking and hydraulic braking of an electrified passenger car", *Proceedings of the Institution of Mechanical Engineers, Part D: Journal of Automobile Engineering* 2012; 226(10): 1289-1302.
3. Sovran, G. and Blaser, D., "Quantifying the Potential Impacts of Regenerative Braking on a Vehicle's Tractive-Fuel Consumption for the U.S., European, and Japanese Driving Schedules," SAE Technical Paper 2006-01-0664, 2006, doi:10.4271/2006-01-0664.
4. Lv, C., Zhang, J.Z., Li, Y.T., Sun D.S. and Yuan, Y., "Hardware-in-the-loop simulation of pressure-difference-limiting modulation of the hydraulic brake for regenerative braking control of electric vehicles", *Proceedings of the Institution of Mechanical Engineers, Part D: Journal of Automobile Engineering* 2014; 228(6): 649-662.
5. Bayar, K., McGee, R., Yu, H., and Crombez, D., "Regenerative Braking Control Enhancement for the Power Split Hybrid Architecture with the Utilization of Hardware-in-the-loop Simulations," *SAE Int. J. Alt. Power*. 2(1):127-134, 2013, doi:10.4271/2013-01-1466.
6. Lagerberg, A., and Bo E., "Backlash estimation with application to automotive powertrains", *Control Systems Technology, IEEE Trans* 2007;15(3): 483-493.
7. Templin, P., "Simultaneous estimation of driveline dynamics and backlash size for control design". Control Applications, IEEE International Conference on, IEEE 2008.
8. Yamaura, H., Ishihama, M., and Togai, K., "Design and Evaluation of Output Profile Shaping of an Internal Combustion Engine for Noise & Vibration Improvement," SAE Int. J. Engines 7(3):1514-1522, 2014, doi:10.4271/2014-01-1683.
9. Baumann, J., Swarnakar, A., Kiencke, U., and Schlegl, T., "A Robust Controller Design for Anti-Jerking," SAE Technical Paper 2005-01-0041, 2005, doi:10.4271/2005-01-0041.
10. Kawamura, H., Ito, K., Karikomi, T., and Kume, T., "Highly-Responsive Acceleration Control for the Nissan LEAF Electric Vehicle," SAE Technical Paper 2011-01-0397, 2011, doi:10.4271/2011-01-0397.
11. Bottiglione, F., Sorniotti, A., Shead, L., "The effect of half-shaft torsion dynamics on the performance of a traction control system for electric vehicles", *Proc. Inst. Mech. Eng. Part D J. Automob. Eng.* 2012; 226(9): 1145-1159.
12. Zhang, J., Lv, C., Yue, X., Li, Y., Yuan, Y., "Study on a linear relationship between limited pressure difference and coil current of on/off valve and its influential factors", *ISA Transactions* 2014; 53(1): 150-161.
13. Lv, C., Zhang, J., Li, Y., and Yuan, Y., "Regenerative Braking Control Algorithm for an Electrified Vehicle Equipped with a By-Wire Brake System," SAE Technical Paper 2014-01-1791, 2014, doi:10.4271/2014-01-1791.
14. Zhang, J., Lv, C., Yue, X., Qiu, M. et al., "Development of the Electrically-Controlled Regenerative Braking System for Electrified Passenger Vehicle," SAE Technical Paper 2013-01-1463, 2013, doi:10.4271/2013-01-1463.
15. Balluchi, A., Benvenuti, L., Di Benedetto, M. D., and Sangiovanni-Vincentelli, A., "The Design of dynamical observers for hybrid systems: Theory and Application to an Automotive Control Problem", *Automatica* 2013; 49(4): 915-925.
16. Balluchi, A., Benvenuti, L., Di Benedetto, M. D., and Sangiovanni-Vincentelli, A., "A hybrid observer for the driveline dynamics," Proceedings of the European Control Conference, 2001.
17. Amann, N., Bocker, J., and Prenner, F., "Active damping of drive train oscillations for an electrically driven vehicle", *Mechatronics, IEEE/ASME Transactions on* 2014; 9(4): 697-700.
18. Lv, C., Zhang, J., Li Y., "Extended-Kalman-filter-based regenerative and friction blended braking control for electric vehicle equipped with axle motor considering damping and elastic properties of electric powertrain", *Vehicle System Dynamics 2014*; 52(11), 1372-1388.

CONTACT INFORMATION

Dr. Lv, Chen
State Key Laboratory of Automotive Safety and Energy
Tsinghua University
Beijing, China
lv-c10@mails.tsinghua.edu.cn

Prof. Zhang, Junzhi
State Key Laboratory of Automotive Safety and Energy
Tsinghua University
Beijing, China
Collaborative Innovation Center of Electric Vehicles in Beijing
jzhzhang@mail.tsinghua.edu.cn

Dr. Li, Yutong
State Key Laboratory of Automotive Safety and Energy
Tsinghua University
Beijing, China
einstein_li@sina.com

Dr. Yuan, Ye
State Key Laboratory of Automotive Safety and Energy
Tsinghua University
Beijing, China
yuanye_yuanye@126.com

ACKNOWLEDGMENTS

The authors would like to thank the Natural Science Foundation of China [Project no. 51475253] and the China Scholarship Council [File no. 201306210121] for funding this work.

DEFINITIONS/ABBREVIATIONS

EV - Electric vehicle

RBS - Regenerative braking system

ICE - Internal combustion engine

CV - Constant-velocity

SMC - Sliding mode control

CO+ - Positive contact

CO- - Negative contact

BL - Backlash

$\mathcal{H}$ - A hybrid system

$\mathcal{H}_O$ - A hybrid observer

DES - Discrete event system

PID - Proportional-integral-derivative